Renewable and Sustainable Energy Reviews 32 (2014) 797–809

Contents lists available at ScienceDirect

Renewable and Sustainable Energy Reviews

journal homepage: www.elsevier.com/locate/rser

A review of icing prevention in photovoltaic devices by surface engineering

R.M. Fillion, A.R. Riahi*, A. Edrisy

Department of Mechanical, Automotive and Materials Engineering, University of Windsor, 401 Sunset Ave., Windsor, ON, Canada N9B 3P4

ARTICLE INFO

Article history:
Received 11 August 2013
Received in revised form
20 October 2013
Accepted 4 January 2014
Available online 11 February 2014

Keywords:
Solar energy
Surface engineering
Icing
Hydrophobic
Self-cleaning
Transparent
Coating
Icephobic

ABSTRACT

The renewable energy sector and the solar industry, more specifically, are expected to grow in the upcoming years. However, in many colder climates worldwide, ice and snow accumulation on solar panels is prevalent and can negatively affect the efficiency or even stop the production of energy. A superhydrophobic coating has been proposed as a functional coating for use in solar cell and outdoor applications. A review of the literature has revealed that a superhydrophobic coating can be designed to display desirable characteristics that can enhance the efficiency of solar cells and prevent the degradation of efficiency over time. Five properties in relation to superhydrophobic coatings have been discussed: ice resistance, transparency, self-cleaning, antireflection, and mechanical robustness. Included in these discussions were the desired effects of the properties, and the parameters needed to optimize these properties. It was found that the water repellent properties of a superhydrophobic coating can prevent and reduce the accretion of ice, while subsequently the ice resistant properties of the composite wetting state can diminish its adhesion, making ice removal a less energy-intensive process. The good resistance to snow accumulation and the self-cleaning capabilities maintain a clean transparent substrate. Additionally, the transparency and intrinsic antireflective effects can be optimized to ensure maximum light transmission and increased efficiency. A stable and mechanically robust coating would allow for minimal maintenance, prolong the benefits of sought after properties, and increase the overall useful life of a solar panel.

Contents

* Corresponding author. Tel.: +1 519 253 3000x3567.
E-mail address: ariahi@uwindsor.ca (A.R. Riahi).

1364-0321/$ - see front matter © 2014 Elsevier Ltd. All rights reserved.
http://dx.doi.org/10.1016/j.rser.2014.01.015

1. Introduction

With advances in technology and the recent shift in mindsets toward sustainability, the renewable energy industry has become a more viable source to meet the energy needs of the world and is being widely researched in all areas [1–5]. In 2010, The U.S. Energy Information Administration's International Energy Outlook reported that renewable energy will be the fastest growing world energy source over the period 2007–2035 [6]. The increase in this demand may be attributed to several factors: the decline in fossil fuels, climate change, and the abundance of renewable energy potential (Table 1). The migration away from fossil fuel usage is an appropriate response to the knowledge that fossil fuel resources are finite and cannot sustain society indefinitely [5,7]. As of 2010, oil production had been nearly static for the past 5 years and marginal productivity was showing signs of stress worldwide [7]. Renewable energy has dawned as a possible solution that may alleviate the growing concerns over greenhouse gas emissions, increasing energy prices, and the dependency on foreign energy sources, and this includes the geopolitical climate that is associated with the production of fossil fuels in some regions of the world [8]. In addition, renewable energy offers the benefits of being clean, abundant, inexhaustible, and for a variety of applications it can even be the most cost-effective source of energy, meeting between 15 and 20% of the total world energy demand as of 2007 [9].

In many places where renewable energy systems are used, climactic conditions are severe and icing is prevalent. This is a problem because the efficiency of wind turbines and solar devices is greatly reduced due to icing and snow accumulation; it may even stop the production of energy all together [1,11–13]. Due to the crippling effect ice accretion has on the ability of solar devices to produce electricity, many researchers have been turning their attention to designing systems of ice removal. The removal of ice can be classified into two categories: active solutions and passive solutions. Active solutions are methods of removing ice after it has been deposited; these include mechanical scraping, thermal treatments, and the use of de-icing fluids. Passive solutions would include treatments that can be applied to a surface prior to its use that would prevent the ice from adhering or cause it to delaminate under its own weight. Active methods are currently widely used, but passive methods have found few industrial uses despite being environmentally friendly, compared to de-icing fluids. Passive methods also represent a cheaper option than active methods which are energy hungry and can be expensive to produce and operate [14]. One such possible passive solution may lie in hydrophobic coatings. Currently, there is no known material that can completely prevent ice or snow from accumulating on its surface; however, some coatings are believed to provide reduced adhesion [15] and for smooth surfaces, there is a clear trend that the ice adhesion strength decreases as the surface becomes more hydrophobic [16].

2. Hydrophobic surfaces

Hydrophilicity refers to the physical property of a material that can transiently bond with water through hydrogen bonding. A water droplet will spread itself on a hydrophilic surface; it may also enter the pores of the material and completely saturate it. Most natural materials are hydrophilic. A water droplet on a hydrophilic surface will occupy as large a surface as possible, thus making the water contact angle significantly low. Hydrophobicity refers to the physical property of a material that repels a mass of water. A water droplet being repelled by the material will not touch a large area of the surface and will take a spherical shape, thus making the water contact angle very large. The evaluation of hydrophilicity and hydrophobicity are made through measuring the angle at which water contacts a surface.

A surface with a water contact angle greater than 90° is usually referred to as hydrophobic, and one with a water contact angle higher than 140° is qualified as ultra-hydrophobic. The surfaces with very high water contact angles, particularly greater than 150°, are usually called superhydrophobic surfaces. The contact angle of water has been commonly used as a criterion to evaluate the static hydrophobicity of a surface, as depicted in Fig. 1. Alone, however, that factor is not adequate for the evaluation of dynamic hydrophobicity, which is the sliding of water droplets. Dynamic hydrophobicity is describing a surface's ability to shed water. Furthermore, to completely describe a superhydrophobic state, the contact angle hysteresis should also be measured. For an optimal superhydrophobic state, the static contact angle should be maximized, and the contact angle hysteresis minimized [17].

2.1. Contact angle hysteresis

The contact angle hysteresis is the difference between the advancing and receding contact angles. The sliding angle and/or the contact angle hysteresis are commonly utilized as criteria for dynamic hydrophobicity on a solid hydrophobic surface [17]. Hysteresis is a phenomenon that can arise from the molecular interactions between the solid and liquid or from irregularities in the surface, such as roughness or heterogeneities. In the case of a sessile drop: when further liquid is added, the contact line advances forward. When the motion of the drop stops it exhibits an advancing contact angle, θ_A. However, if liquid is removed from the sessile drop, the contact angle decreases before the contact line retreats back to a receding value, θ_R. The contact angle hysteresis is referred to as the difference between θ_A and θ_R. Furthermore, in the case of a droplet moving along the solid surface, the contact angle that appears at the front of the droplet, θ_A, will be greater than that at the back of the droplet, θ_R. This is due to roughness and surface heterogeneity, resulting in the contact angle hysteresis [18,19].

2.2. Origin of hydrophobic surfaces

The phenomenon of hydrophobicity and self-cleaning surfaces was observed for the first time in nature. The term “Lotus effect” is accredited to the botanist Wilhelm Barthlott [20,21] and refers to a special ability of the Lotus. The Lotus flower can stay clean and unaffected by dirt and pollution, even when growing in muddy waters. The Lotus leaf's “self-cleaning” surface, which reaches water contact angle values greater than 150°, is hydrophobic and rough. Its surface is composed of two layers, a lower layer of micro-sized roughness covered by a second waxy layer of hydrophobic crystalloids of nano-sized roughness. The self-cleaning mechanism is characterized by three properties: superhydrophobicity, low sliding angle, and removal of dirt particles by the sliding droplet [22]. The amazing functions and capabilities of the Lotus, like other biological species, have developed over millions of years through evolution (Fig. 2). The ambition to recreate biological systems found in nature has sparked interest in a wide range of research and has led to the

Nomenclature

E	energy required to form a unit of the solid-liquid interface
f	contact area fraction
g	gravitational acceleration
K_R	the interfacial adhesion parameter
m	mass of water droplet
q	charge on ice surface
q'	image charge
r	roughness factor
S_1	the energy content of a measured unit area before wetting
S_2	the liquid surface tension
S_{12}	the energy content of a measured unit area after wetting
W	width of water droplet

Greek Symbols

α	sliding angle
α'	sliding angle for a rough surface
γ_{LV}	interfacial free energy per unit area of the liquid-gas interface
γ_{SL}	interfacial free energy per unit area of the solid-liquid interface
γ_{SV}	interfacial free energy per unit area of the solid-gas interface
ε	dielectric constant
θ	water contact angle
θ'	water contact angle as measured on a rough surface
θ_A	advancing contact angle
θ_R	receding contact angle
ρ	density of liquid
σ_1	the total area of the solid-liquid interface
σ_2	the total area of the liquid-air interface

development of advanced functional materials or devices that can be found in the literature: A dye-sensitized solar cell mimics the photosynthesis process [23,24], a specialized adhesive surface mimics a gecko's foot or a mussel's ability to adhere to wet surfaces [25–29], a photonic crystal mimics the wings of a butterfly [30–34], an anti-reflective coating mimics the eyes of a moth [35–37], and a superhydrophobic and self-cleaning surface mimics the surface of a Lotus leaf, water strider's leg and a cicada orni's wing [38–49].

2.3. Progressive theories on surface wettability

The thermodynamics between a liquid and a solid was described by Young in 1805 [50]. His paper explained the wetting phenomenon for smooth surfaces and the forces causing liquids and solids to behave in a predictable manner. Though not appearing in his publication, this equation is attributed to him.

$$\cos\ \theta = (\gamma_{SV} - \gamma_{SL})/\gamma_{LV} \tag{1}$$

where γ_{SL}, γ_{SV}, and γ_{LV} are the interfacial free energies per unit area of the solid–liquid, solid–gas, and liquid–gas interfaces respectively.

Wenzel [51,52] proposed a modification to Young's equation after he observed the effect of surface roughness on the contact angle of water. His modification included a roughness factor, r, which is defined as the ratio between the actual rough surface area and the geometric projected area. Wenzel's equation can predict that a solid hydrophilic substrate will experience increased wetting, or a lower contact angle, due to roughness on its surface. However, a solid hydrophobic substrate will experience less wetting, or a higher contact angle, due to surface roughness.

$$rA = r(S_1 - S_{12}) = S_2\ \cos\ \theta \tag{2}$$

where r is a roughness factor, A is the adhesion tension, S_2 is the surface tension of the liquid, and S_1 and S_{12} are the energy contents of a measured unit area before and after wetting respectively.

The theories of Young and Wenzel could be applied to a chemically homogeneous surface, but not to a non-homogeneous surface. It was Cassie and Baxter [53,54] who extended the work of Wenzel to include non-homogeneous and porous surfaces. The Cassie–Baxter equation represents a contact angle at a surface that is composed of both solid and air because the liquid is prevented from fully penetrating into the pores of the surface due to its inherit repellence towards it which leaves air trapped in the roughness morphology.

$$\cos\ \theta = -\frac{E}{\gamma_{LV}} = \sigma_1\ \cos\ \theta_1 - \sigma_2 \tag{3}$$

where E is the energy gained by forming a unit area of the solid–liquid interface, γ_{LV} is the liquid–gas interfacial energy, and σ_1 and σ_2 are the total areas of the solid–liquid interface and the liquid–gas interface respectively. These three theories can be grasped visually with the aid of Fig. 3 [55].

2.4. Influence of roughness

Superhydrophobic surfaces require both low surface energy and the appropriate surface roughness [48,56]. Hare et al. [57] showed that fluorinated surfaces create the lowest polymer surface energies, resulting in highest contact angles. Nishino et al. [58] furthered this work by demonstrating that regularly aligned and close-packed CF_3 groups attain the lowest surface free energy of any flat solid. This surface exhibited a contact angle of 120° and contact angle higher than this can only be obtained by roughening the surface [59]. Roughness can enhance hydrophobicity and decrease resistance to the flow with the correct factors considered [19]. The roughness of the coating should be hierarchical as that of the lotus leaf, with micro-scale roughness and nano-scale roughness to achieve best results (Figs. 4 and 5) [19,60–63]. For most superhydrophobic surfaces, it is important that a composite solid–liquid–air interface is formed. A composite interface drastically decreases the adhesion of a droplet to the solid surface and contact angle hysteresis by decreasing the area of contact between the liquid and solid [61].

A composite state is essential for superhydrophobicity. Therefore, in the design of a superhydrophobic surface, the stability of the composite state should be addressed. With better knowledge of the parameters affecting the hydrophobicity of a surface, new models are being formed. Rios et al. [64,65] proposed an equation to create a more comprehensive definition of a hydrophobic

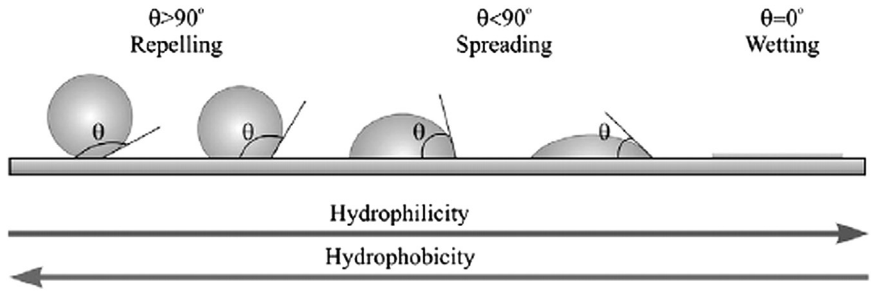


Fig. 1. The wettability of a surface can be determined by the water contact angle measured. (Reprinted with permission from [55]. Copyright 2009 Elsevier.).

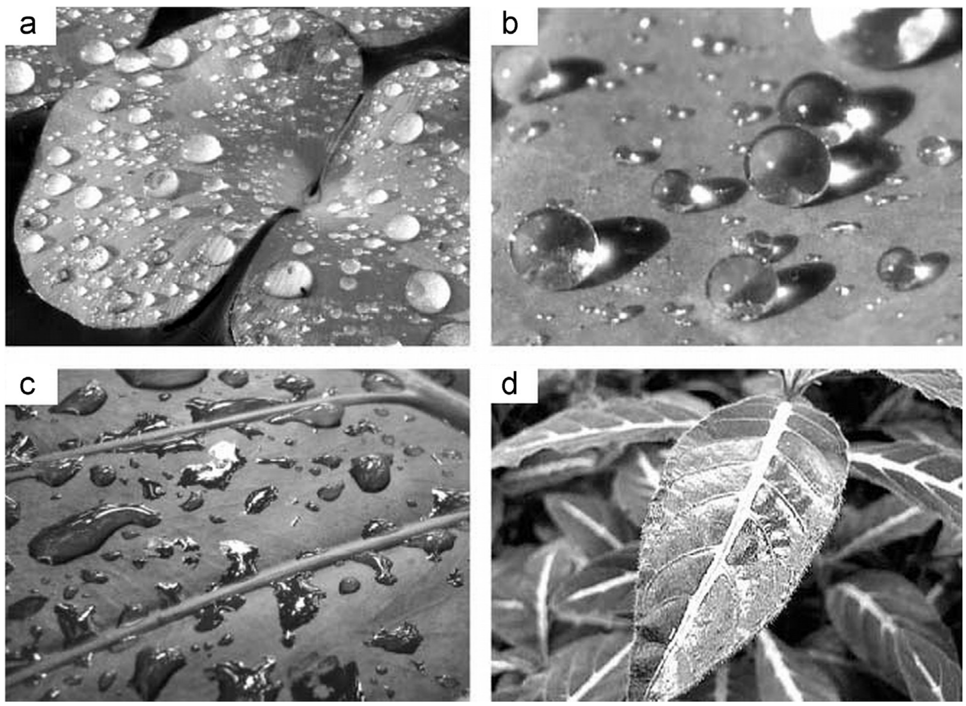


Fig. 2. Examples of surface wettability in nature, (a) the hydrophobic leaves of the *Regnellidiumdiphyllum*, (b) *Brassica oleracea* leaves show superhydrophobicity, (c) the *Alocasiaodora* has hydrophilic leaves, and (d) the superhydrophilic leaves of the *Ruelliadevosiana*. (Reprinted with permission from [40]. Copyright 2009 The Royal Society.).

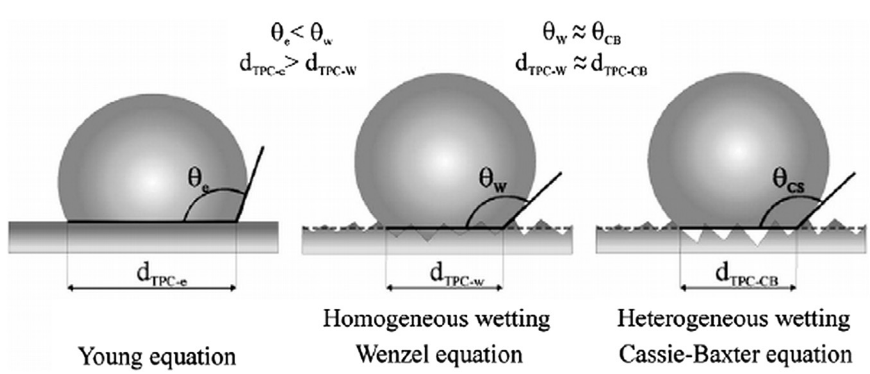


Fig. 3. Schematic of progressive theories on surface wettability: Young's theory, Wenzel's theory and Cassie–Baxter's theory. (Reprinted with permission from [55]. Copyright 2009 Elsevier.).

surface that includes the effects of both the contact and sliding angles.

$$\sin\,\alpha' = \frac{K_R \pi f}{g}\left[\frac{3}{\rho\pi(2-3\,\cos\,\theta' + \cos^3\theta')}\right]^{2/3} \sin^2\theta' m^{1/3} \tag{4}$$

where α' is the sliding angle for a rough surface, θ' is the contact angle, and f is the contact area fraction. KR represents the interfacial adhesion parameter, g is the gravitational acceleration, ρ is the density of the liquid, and m the mass of the droplet. Since Sinα' is proportional to f, this equation demonstrates that the rougher the hydrophobic surface is, the smaller f will become and thus the lower the sliding angle will be. It also indicates that as the roughness scale is decreased into the nano-scale, the sliding angle will be at its lowest.

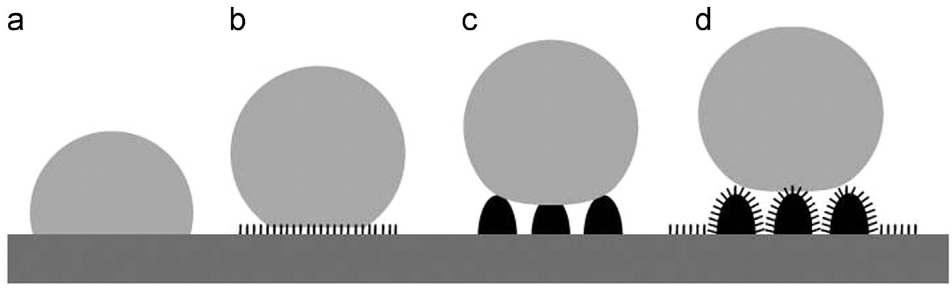


Fig. 4. Schematic displaying the different roughness regimes, (a) smooth surface, (b) nano-roughness, (c) micro-roughness, and (d) a combination of micro- and nano-roughness (hierarchical roughness). (Reprinted with permission from [63]. Copyright 2009 The Royal Society.).

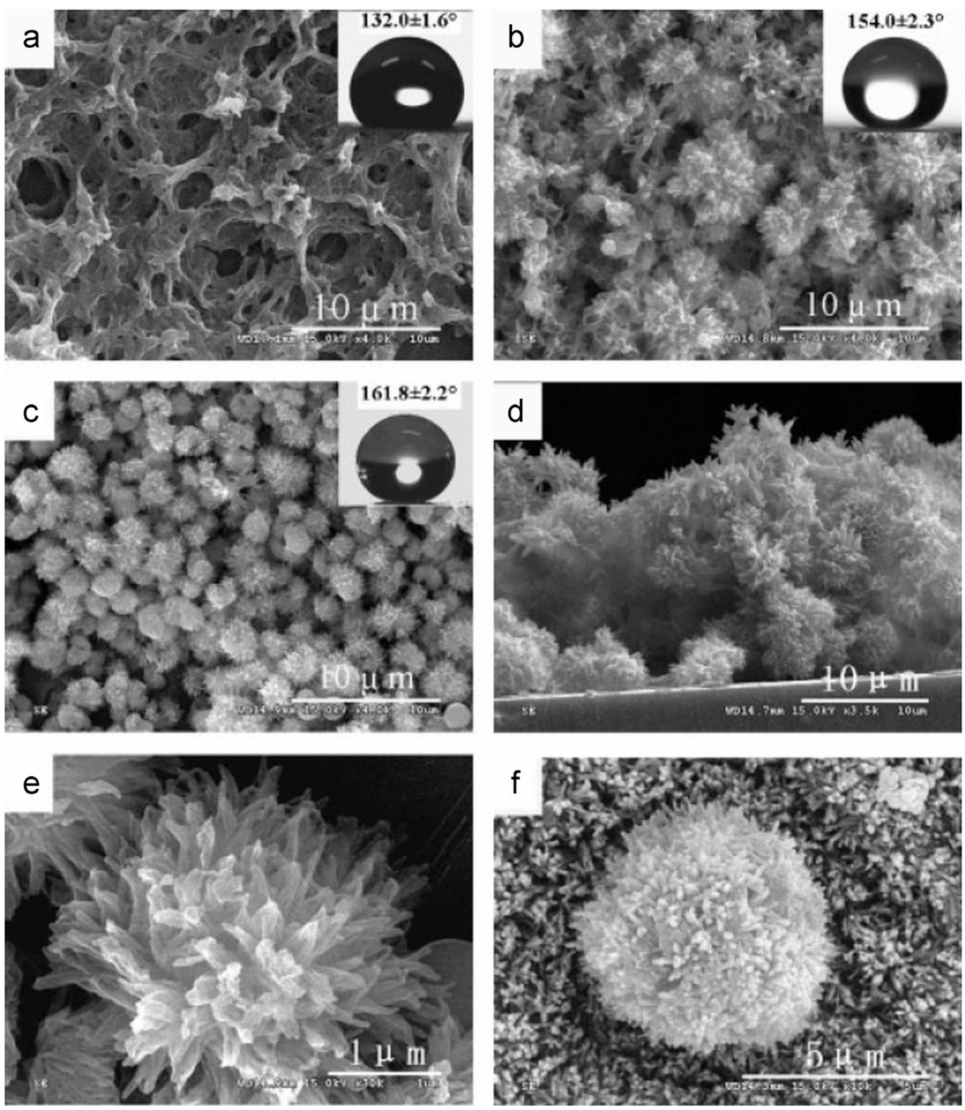


Fig. 5. Scanning electron microscope (SEM) images of biomimetic hydrophobic coatings, (a–c) increased hierarchical roughness displays higher water contact angles, (d–e) close up images of fabricated coating, and (f) a single papilla on a natural lotus leaf. (Reprinted with permission from [62]. Copyright 2005 John Wiley and Sons.).

2.5. *Deposition of coating*

To date, many methods have been explored for the deposition of thin coatings with special wettability including chemical vapor deposition [66–69], sol–gel technique [70–77], plasma etching [78–81], the utilization of templates [40,48,49,82,83], spray pyrolysis technique [84–86], layer-by-layer deposition [87–89], and lithography [90–93]. When choosing a process for the deposition of hydrophobic coatings for industrial use, one should consider the monetary cost, the simplicity, and the ability of a process to be expanded for large-scale manufacturing. Some simple and inexpensive methods would include the sol–gel technique, spray pyrolysis, and layer-by-layer deposition. Patil [86] has demonstrated that spray pyrolysis technique has several advantages over other methods. These include simplicity, safety, low cost of apparatus and raw materials, as well as large-scale deposition. Additionally, the layer-by-layer technique is capable of depositing the desired coating compositions on many different surfaces,

including flat and rough surfaces of large areas, and has been shown to be simple, inexpensive, and versatile [87].

3. Coating design

3.1. Icephobicity

The design of an effective ice resistant coating for use in the solar industry would require the optimization of multiple factors as well as its ice resistance properties. The overall factors that need to be considered are the ice resistant properties, transparency, self-cleaning capabilities, antireflective effects, and the durability of the coating. A fully optimized superhydrophobic coating would show great promise for maintaining the efficiency of solar devices by preventing the accumulation of ice, snow, dirt, and dust.

3.1.1. Ice nucleation

In order to properly discuss the ice resistant properties of hydrophobic coatings, it is necessary to understand the nucleation of ice on a solid surface and its adhesion to that surface. A small amount of liquid that has been cooled below its equilibrium temperature will not freeze immediately, but will be in a metastable supercooled state for some amount of time. Because it is energetically favorable for a supercooled liquid to crystallize, only a limited degree of supercooling can be achieved before spontaneous crystallization of the liquid into ice will occur. During the freezing process, a very small volume of liquid must crystallize and grow until all the liquid is frozen because freezing is a continuous process [94]. If a small crystal embryo grows on an insoluble foreign surface or particle to increase its stability, the nucleation process is termed heterogeneous. Homogeneous nucleation would take place within the pure liquid itself if there are no foreign surfaces or particles for the crystal embryo to grow upon. In heterogeneous nucleation, the growth of an ice-like cluster that is bounded on one side by a foreign surface will be promoted because it will have a lower free energy than a cluster that is independent. When the crystal embryo has crystallized, the growth of the crystal can occur [94]. It is the same process of supercooled water droplets within the atmosphere making contact with a surface and nucleating as ice crystals that accounts for atmospheric icing events [95]. Ice deposited on a surface can exist in different variations; when there is no liquid layer and no run-off when the ice is being deposited, the icing process is called 'dry growth' and the resulting ice is referred to as 'rime'. However, it is called 'wet growth' if there is a liquid layer on the surface of the accumulated ice and freezing is taking place beneath this layer, resulting in ice referred to as 'glaze' [96].

3.1.2. Ice adhesion

Preventing ice from forming on surfaces at sub-zero temperatures may be accomplished by producing coating materials that are icephobic in nature. Therefore, understanding of the ice–solid interface should be considered an important aspect in achieving icephobic surfaces. The mechanisms involved in ice adhesion are often complex and involve the nature of the substrate, the ice, and the mode of fracture. The adhesion of ice will differ from one type of substrate to another, such as a polymeric material to a metal. If water has been frozen to a metallic surface, the interface created is stronger than the shear strength within the ice which will result in fractures occurring within the ice itself. However, when water is frozen onto a polymeric surface, the interface created is weaker than the shear strength within the ice and failure can now occur at the interface [97]. A superhydrophobic coating can both decrease and prevent ice accumulation, and reduce the adhesion of any ice that forms on its surface. Superhydrophobic coatings can prevent and decrease ice accumulation by delaying freezing time [98–101] and by shedding the water on its surface before it can freeze [100–102]. There are two explanations for the ability of a superhydrophobic coating to delay the onset of freezing. Tourkine et al. [100] proposed that it was due to the layer of air in the voids of the rough superhydrophobic coating that creates a thermal barrier which insulates the liquid from the surface, thus delaying freezing. Additionally, Alizadeh et al. [99] suggested that the delayed freezing, or reduction of macroscopic nucleation rate, is caused by both a reduction of the water-substrate interfacial area and an increase in nucleation activation energy which are characteristic of high contact angles. However, this relationship does not hold true at lower supercooling temperatures. Wang et al. [103] demonstrated that a superhydrophobic coating can not only be effective in delaying the start of icing, but also in increasing the whole icing process time compared with the plain surface under the same experimental conditions. In addition, the morphology and composition of the iced solid surface plays an important role. For a superhydrophobic coating, as the contact area of water is negligible, such a surface would reduce the contact area of ice on the surface and should significantly reduce the adhesion of ice [70].

In ice adhesion research, a common theme has been to compare the contact angle, or wettability, of a surface with the adhesion of ice to that surface. This is often plotted as ice adhesion strength as a function of the water contact angle; however, researchers have seen that data presented in this way does not always follow expected trends. In some cases, researchers have reported that the ice adhesion decreases with an increasing water contact angle, and others have found insufficient relation between the two parameters [104]. It was later shown that the ice adhesion strength on a rough hydrophobic surface is not correlated with the water contact angle but is correlated with the contact angle hysteresis, or dynamic hydrophobicity. It was also shown that despite the rough surface of a superhydrophobic coating, it will reduce the adhesion of ice more than a smooth hydrophobic surface of the same chemical composition, and superhydrophobic coatings exhibiting a contact angle hysteresis lower than 5° lead to very high icephobic properties [15,105,106]. The continuing research in the ice resistance of superhydrophobic coatings further revealed that only the receding contact angle was important in matters of ice adhesion [107]. Meuler et al. [104], after testing 22 surfaces of varying wettability, concluded that ice adhesion is related to the receding contact angle of the surface and by minimizing the receding contact angle the ice adhesion would also be reduced. Nosonovsky and Hejazi [107] further showed that a composite, or Cassie–Baxter, wetting state introduces voids between the solid surface and the ice which serve as stress concentrators, or microcracks, thereby decreasing the adhesion of ice. They showed that it was the size of the microcracks at the interface that is the critical parameter that will govern the adhesion of ice to a superhydrophobic surface even though high receding angles are well correlated with reduced ice adhesion. This can help to explain why some superhydrophobic surfaces can result in strong ice adhesion if they do not provide sufficiently large voids at the interface. The stability of a superhydrophobic coating in the Cassie–Baxter wetting state is also an important factor that needs to be considered. In a humid atmosphere, when water condenses in the rough structure of the coating, the contact angle of water will decrease as the droplet switches from a Cassie–Baxter state to a Wenzel state. If a droplet freezes in this condition, it may lead to very large values of ice adhesion called the anchor effect [108]. Ice exhibits a very strong adhesion to materials which is largely due to the polar ice molecules strongly interacting with the solid surface. There are three physical mechanisms involved in the adhesion of ice to a surface, specifically, hydrogen bonding, van der Waals forces, and direct electrostatic interactions. Of these three, the direct electrostatic interactions have been found to be

the dominant factor [109,110]. Charges on ice induce equal and opposite charges on metals, whereas on dielectrics, the induced charge is smaller and is related to the dielectric constant by the following equation:

$$q' = q\frac{\varepsilon - 1}{\varepsilon + 1} \quad (5)$$

where q' is the image charge induced by a charge q on the ice surface and ε is the dielectric constant of the insulating material on which ice is deposited [109]. Therefore, the interacting force between ice and a metal is greater than that between ice and a dielectric material. Based on the previous equation, materials with a very low dielectric constant would significantly reduce the adhesion of ice by reducing the electrostatic interaction [14,70,110].

Another physical factor that may affect the adhesion of ice to a superhydrophobic coating is particle size. Cao et al. [111] developed superhydrophobic coatings on aluminum substrates (Fig. 6) and determined that the critical particle sizes that determine the superhydrophobicity of the coating and the ice resistant property respectively are in two different length scales. The hierarchical coatings were made with particles up to 10 μm in diameter for the micro-roughness regime which rendered them all superhydrophobic. The anti-icing properties of these coatings, however, are distinctly different. No ice formed on the samples when particles of 20 and 50 nm were used for the nano-scale roughness regime, but the probability of icing increases remarkably when the particle diameter is larger than 50 nm. They show that it is uncertain whether a superhydrophobic surface can be ice resistant without having a detailed knowledge of the surface morphology and caution should be taken when the ice resistant properties are correlated to the superhydrophobicity.

3.1.3. Moisture condensation

Dew condensation is commonly observed in nature. When the air temperature drops below the dew point, water vapor in the air becomes liquid and condensation occurs. At the dew point, there is a change of the interfacial free energy of the solid–gas interface by water adsorption and the contact angle decreases which suggests an unstable composite state, or mode transition from Cassie–Baxter to Wenzel [112]. As the temperature of some superhydrophobic surfaces is lowered past the dew point, they display sudden and undesirable decreases in the receding water contact angles. The observed decrease in water contact angle indicates a transition from the Cassie–Baxter state to the Wenzel state, likely due to the capillary condensation of liquid water in the crevices of the textured surface [113]. For a surface to be effectively icephobic it must be able to resist transitions to the fully wetted state which may be caused by the condensation of moisture from the ambient atmosphere or by the kinetic energy of falling rain droplets [114].

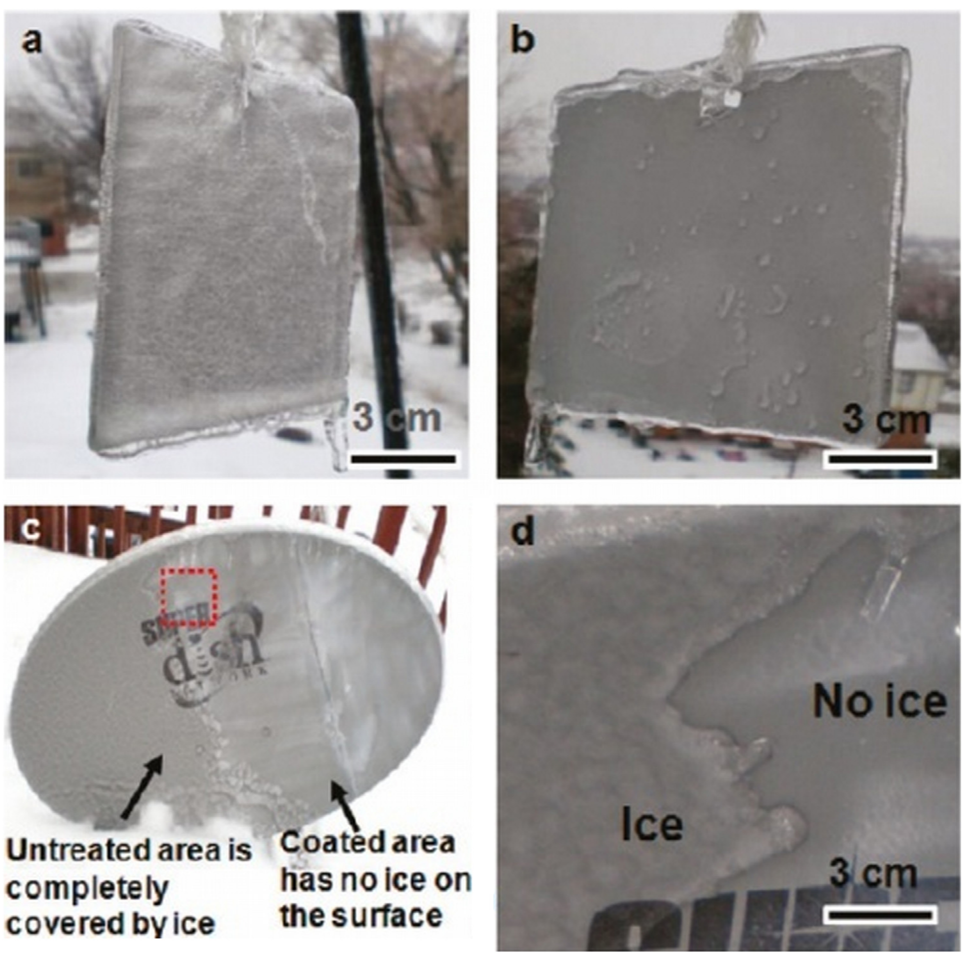


Fig. 6. Test of anti-icing properties in naturally occurring “freezing rain“. (a) Untreated side of an aluminum plate after the natural occurrence of “freezing rain“. (b) Treated side of the aluminum plate coated with a superhydrophobic composite after the “freezing rain”. (c) Satellite dish antenna after the freezing rain. The left side is untreated and is completely covered by ice, while the right side is coated with the superhydrophobic composite and has no ice. (d) Close-up view of the area labeled by a red square in (c), showing the boundary between the coated (no ice) and uncoated area (ice) on the satellite dish antenna. (Reprinted with permission from [111]. Copyright 2009 American Chemical Society.).

In contrast, however, Wang et al. [115] developed a superhydrophobic coating that maintains contact angles above 150° in temperature ranges from −10 to 17.5 °C.

It is not always the case that water vapor forms a liquid condensate once undergoing a phase transition on a supercooled surface. Frosting, which is the process of water desublimation onto a surface and forming small ice crystals, may also happen. Varanasi et al. [16] demonstrated that frost formation could significantly compromise the icephobic properties of superhydrophobic surfaces. They used an environmental scanning electron microscope to take snapshot images of the nucleation and growth of frost on the superhydrophobic surfaces. It was shown that indiscriminate frost formation cannot be avoided on surfaces comprised of spatially uniform intrinsic surface energy (Fig. 7) once the necessary supersaturation conditions are achieved. The formation of frost can result in the loss of the superhydrophobic state and complete saturation of the surface morphology by frost which will lead to an increased ice–substrate contact area, and thus to increased ice adhesion and the loss of icephobicity. It was concluded that superhydrophobic textures will increase the adhesion of ice whenever frost can form indiscriminately on the surface. These findings are important to the consideration of superhydrophobic protective coatings for solar applications in climates that experience freezing temperatures at night which result in frosting. Controlling the condensate nucleation spatially offers one possible route for overcoming the frost-driven transition into the Wenzel state. It may be possible to form weakly adhered composite ice if the nucleation of ice is constrained to the upper regions of the surface texture and prevent forming the strongly adhered Wenzel ice [117]. Although frost formation will occur when the temperature of a surface is below the freezing point of water and exposed to humid air, just like the freezing of water, frost formation on a superhydrophobic coating can be delayed. Liu et al. [116] demonstrated that a superhydrophobic coating with a CA of 162° was able to delay frost deposition for 55 min, compared with the uncoated sample. Additionally, Cai et al. [117] tested frost growth on a normal copper surface as well as one with a hydrophobic coating and found frost appeared

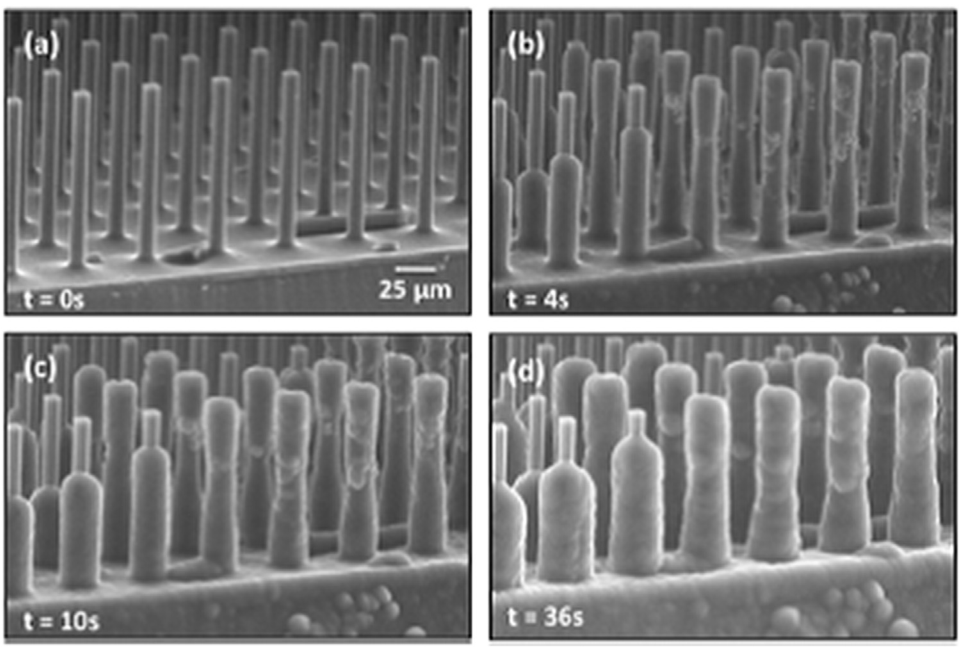


Fig. 7. SEM images of frost formation on a superhydrophobic surface. (Reprinted with permission from [16]. Copyright 2010 American Institute of Physics.).

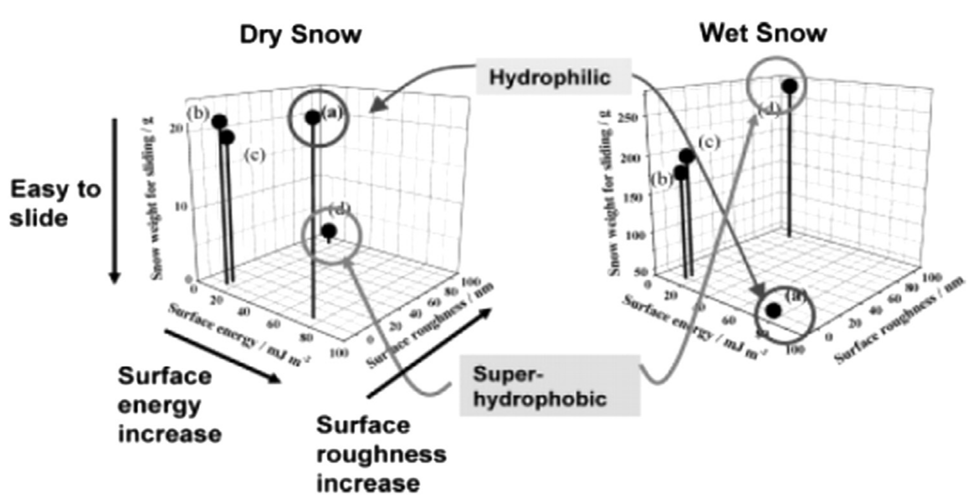


Fig. 8. Relationship between hydrophobicity and maximum snow weight for sliding on various hydrophobic surfaces: (a) normal glass surface; (b) glass surface coated with fluoroalkylsilane; (c) glass surface coated with both colloidal silica and fluoroalklsilane; (d) superhydrophobic film surface. (Reprinted with permission from [17]. Copyright 2004 Journal of the Ceramic Society of Japan.).



Fig. 9. Photograph of water droplets on F-SiO2 NP-coated glass substrate. (Reprinted with permission from [126]. Copyright 2012 American Chemical Society.).

on the hydrophobic coating surface later with lower frost height, sparse distribution, and less aggradations of ice crystals than that on the normal copper surfaces.

3.1.4. Snow adhesion

Another important factor in the design of a superhydrophobic coating for use in freezing climates is the adhesion of snow to its surface. Snow is generally a mixture of ice and water and its adhesion to surfaces is affected by many factors such as the surface's roughness and composition, as well as the atmospheric temperature and wind velocity. The temperature of the ground also alters the adhesion behavior of snow as the ground temperature affects the water content of snow, below -1 or $-2\,^{\circ}$C the snow is dry but above that, a thin layer of water covers the ice, creating wet ice with properties between that of ice and water. Due to the difference in water content, dry snow exhibits different sliding or adhesion behaviors than wet snow [17]. Various investigations have examined the adhesion behavior of snow on a solid surface. Nakajima demonstrated that a superhydrophobic coating showed an excellent anti-snow adhesion property against both dry and wet snow along with acceleration of sliding of dry snow (Fig. 8) [17]. Other studies have found poor sliding behavior of wet snow on superhydrophobic surfaces [118].

3.1.5. Evidence of icephobic characteristics

Although much research is being performed in this field, not everyone agrees. Chen et al. [119] disagree that a superhydrophobic (rough) surface can decrease ice adhesion. In their experiment, the superhydrophobic surfaces displayed ice adhesion values near superhydrophilic surfaces; this was determined to be caused by mechanical interlocking from water penetrating the roughness of the microstructure. The cause of the water penetration was related to the cold temperature. When water rests on a superhydrophobic surface at room temperature, it is in a composite state and the liquid water is in thermodynamic equilibrium with the air trapped in the roughness of the surface beneath the liquid. If the temperature of the surface is lowered, it becomes more hydrophilic as the water molecules adsorb at the walls of the surface textures. Simultaneously, water condensation occurring on the inside the surface texture drives a transition from a composite state to the Wenzel state. When water freezes in the Wenzel state, the ice and the surface texture are mechanically interlocked, resulting in large increases in ice adhesion strength. Despite some disagreements on the icephobicity of a superhydrophobic coating, there have been many studies of superhydrophobic coatings exhibiting drastically reduced ice adhesion [14,15,102–107,110,120–123]. Dodiuk et al. [124] developed a superhydrophobic coating that reduced the ice adhesion by 18 times when compared to bare aluminum and

Table 1
The potential resources of global renewable energy [10].
Source: U.S. Energy Information Administration (July 2010).

Usable global renewable energy resources (exajoules per year)			
Resource	Current use	Technical potential	Theoretical potential
Hydropower	10.0	50	150
Biomass energy	50.0	> 250	2900
Solar energy	0.2	> 1600	3,900,000
Wind energy	0.2	600	6000
Geothermal energy	2.0	5000	140,000,000
Ocean energy	–	–	7400
Total	62.4	> 7500	> 143,000,000

Sarkar et al. [70] developed a superhydrophobic coating and froze small cylinders of water to the surface using a mold and tested the adhesion of ice. The untreated aluminum surface showed an ice adhesion strength of 369 ± 89 kPa, whereas the ice debonded spontaneously on its own from the superhydrophobic surface.

3.2. Transparency

It has been shown that with proper consideration and understanding of the mechanisms of ice adhesion and the prerequisite surface properties, it is possible to minimize ice–substrate interactions and facilitate the successful development of an ice resistant coating. Equally important consideration should be given to the transparency of the superhydrophobic coating if it is to be utilized for solar applications. The notion of coupling superhydrophobicity and transparency is counterintuitive since the optimization of superhydrophobicity involves maximizing surface roughness, and the increased feature size, either from particles or through induced roughness, results in increased light scattering [125]. In general, transmittance of light through the coating decreases with increasing roughness, especially if the roughness exceeds the wavelength of light [37]. However, despite the challenges associated with developing a transparent superhydrophobic coating, many have been reported in the literature (Fig. 9) [17,56,59,66,72–75,76,77,84,85,87,89,126–135]. In order to sustain optical transparency in the visible light range (wavelength of 380–760 nm), the roughness of the coating surface should either be much lower than this range, or much higher (less than 80 nm or more than a few microns) [17]. Reports of superhydrophobic coatings with visible light transmittance of over 90% are not unheard of [72,132,133] and some have reached transmittances of over 98% for wavelengths longer than 590 nm [89,134]. Thus, it is apparent that with an optimized superhydrophobic coating a solar cell's performance can remain unaffected due to the effects of light scattering [127].

3.3. Self-cleaning

Another beneficial property of a superhydrophobic coating is their self-cleaning capability. A coating that has self-cleaning properties is important in order to prevent efficiency degradation of the solar device by the accumulation of dirt and dust on the coating surface [136,137]. Both hydrophilic and hydrophobic surfaces exhibit self-cleaning properties through the nature of the interaction of water on the surface The former does this by creating sheets of water that carry dust and dirt as it flows; the latter by rolling droplets (and entrapped dust and dirt) off the surface [136–138]. Not every superhydrophobic surface exhibits self-cleaning properties; there are some important factors that need to be taken into consideration to ensure the desired self-cleaning characteristics. When considering self-cleaning surfaces, the factor of water drop adhesion to the surface is paramount.

A common method used to characterize the adhesion of a water droplet to a surface is to use the critical tilting angle, or sliding angle. When a droplet of known weight is placed on a surface and tilted; the point at which the weight of the droplet overcomes the adhesion to the surface and slides off is referred to as the critical tilting angle [59]. In the case when a superhydrophobic surface is prepared by coating hydrophobic materials directly onto hydrophilic ones, the coating homogeneity is very important. Any remaining hydrophilic material exposed on the surface will become an anchor site for the water droplets due to their affinity for water. If this is the case, even if the apparent contact angle is sufficiently large, the sliding angle will be increased dramatically. Generally, the effects of coating heterogeneity are less conspicuous on the static contact angle of water than on the sliding behavior [17].

3.4. Antireflection

Many nanostructured surfaces have intrinsic antireflective properties and this has promoted the convergence of antireflective structures with self-cleaning structures which could be used in solar devices and other outdoor optical applications [76,87,127–129,133,134,139–146]. Due to the high refractive index of the material surfaces in conventional solar cells and panels, up to 30% of incident light can be reflected back and dust and moisture accumulation can scatter an additional 10% [147]. Some superhydrophobic coatings have antireflective capabilities because the light being reflected from the coating–substrate and coating–air interfaces is subject to descructive interference, resulting in high optical transmission and low reflectivity [128].

Antireflective surfaces can not only improve the transparency of optical devices through improving the light transmittance ratio [76,131,133,134,148] (Fig. 10), but also improve the photovoltaic conversion efficiency of solar cells [149,150]. Two of the most crucial physical parameters in designing an antireflective coating are the thickness of the coating, and its refractive index [149]. Suppressing reflection over a broad spectral range can be accomplished by forming a gradual transition of the refractive index by subwavelength antireflective structures and gradual transition in the refractive index is generally regarded as the preferred way to achieve the perfect antireflective effect [37,151]. Furthermore, the hierarchical roughness of a superhydrophobic coating is advantageous over a smooth hydrophobic coating due to the decreased angle dependence on its antireflective property [151]. From literature, more sources can be found that show an antireflective coating can increase the efficiency of a solar cell [134,152,153]. Minemoto et al. [149] were able to increase the average conversion efficiency of Si solar cells by 25% (relative) by applying ZnO antireflective coatings and Prevo et al. [154] increased the efficiency by 10% (relative) with the use of their antireflective coating.

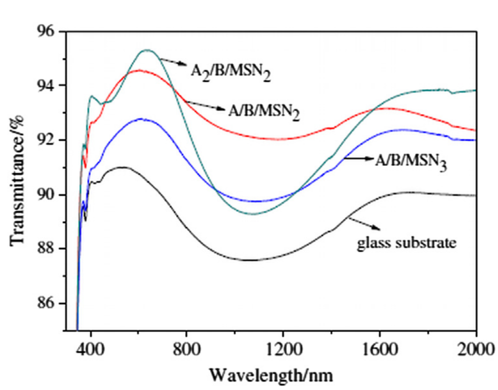


Fig. 10. Transmission spectra of glass substrate and glass substrates coated with broadband antireflective superhydrophobic A/B/MSN_2, A/B/MSN_3 and A_2/B/MSN_2 coatings in the wavelength range of 400–2000 nm. (Reprinted with permission from [133]. Copyright 2013 Elsevier.).

3.5. Durability

Lastly, the durability of the superhydrophobic coating should be taken into consideration. The durability and mechanical robustness of the coating are particularly important to consider because the fragile hierarchical roughness can be irreversibly destroyed, which will inevitably lead to an increase in the contact angle hysteresis and a rapid decrease in the static contact angle [155]. The outdoor testing of coatings with special properties (superhydrophobicity, self-cleaning, and antireflection) is necessary to evaluate their degradation when they are exposed to the natural environment because long periods of exposure to dirt, light, abrasion, and other factors that are typically experienced outdoors. These natural factors contribute to the degradation in the following ways: the decomposition of the hierarchal roughness structure, the accumulation of strains adhering to the surface, and the gradual removal of the water-repellent agents from the surface [17]. Although a rough superhydrophobic coating is sensitive to degradation, many improvements have been made to increase its durability [156–159] and new self-healing superhydrophobic surfaces are being created [158]. Sasaki et al. [160] reported that the formation of an indium-tin oxide (ITO) layer on the surface of the base-film will decrease the surface electric resistance and improve the durability of superhydrophobicity during exposure outdoors. Additionally, Nakajima et al. [161] reported that the addition of only a small fraction of TiO_2 photocatalyst provides an effective self-cleaning property to superhydrophobic coatings and maintains high contact angles during long periods of outdoor exposure. Subsequently, superhydrophobic coatings with desirable mechanical properties have been reported in the literature. Menini et al. [121] developed a superhydrophobic coating that was able to reduce the adhesion of ice to aluminum by four times and after 14 ice-shedding events using an aggressive centrifugal technique, the icephobicity was unaffected. Deng et al. [127] reported a transparent superhydrophobic coating that was able to undergo adhesion tape peeling tests and sand abrasion, but still retain its superhydrophobic properties. Boinovich et al. [162] developed a durable icephobic coating for stainless steel that after 100 icing/deicing cycles, which were accompanied by mechanical stresses, long-term contact with water and saturated vapor, was still demonstrating multimodal roughness, low surface energy, and stability of the superhydrophobic state. In addition to mechanical properties, there have been other properties reported that are sought after in the design of a superhydrophobic coating for outdoor applications. Wang et al. [163] demonstrated a transparent superhydrophobic nanostructured coating that was able to withstand extended exposure to UV illumination without a significant loss of hydrophobic properties, which favors outdoor self-cleaning applications. Kavale et al. [56] reported a transparent superhydrophobic coating that had undergone a humidity test in which the coating was subjected to a relative humidity of 90% at 30 °C for a period of 45 days. After completing the test, the coating exhibited a decrease of only 2° in its water contact angle, from $171 \pm 1°$ to 169°. This slight drop in water contact angle was determined to be caused by a slight adsorption of moisture from the atmosphere; when the samples were dried in an oven, their contact angles returned to their original values. Finally, Hou et al. [38] developed a stable polytetrafluoroethylene superhydrophobic surface which could be immersed in water for long periods of time without affecting the water contact angle, demonstrating the coating's hydrophobic stability.

4. Summary

In conclusion, a superhydrophobic coating can be designed to display desirable characteristics that can enhance the efficiency of solar devices and prevent the degradation of efficiency over time. Five properties in relation to superhydrophobic coatings have been discussed: ice resistance, transparency, self-cleaning, antireflection, and mechanical robustness. Included in these discussions were the desired effects of the properties, and the parameters needed to optimize these properties. It was found that:

- The water repellent properties of a superhydrophobic coating can prevent and reduce the accretion of ice. Subsequently, the ice resistant properties of the composite wetting state can diminish its adhesion, making ice removal a less energy intensive process.
- The good resistance to snow accumulation and the self-cleaning capabilities maintain a clean transparent substrate.
- The transparency and intrinsic antireflective effect can be optimized to ensure maximum light transmission and increased efficiency.
- A stable and mechanically robust coating would allow for minimal maintenance, prolong the benefits of the sought after properties, and increase the overall useful life of a solar device.

Acknowledgments

The authors are grateful to the Natural Science and Engineering Council of Canada (NSERC) for providing financial support. The authors would like to thank Ms. Simina Fillion for editing the manuscript.

References

[1] Carriveau R, Edrisy A, Cadieux P, Mailloux R. Ice adhesion issues in renewable energy infrastructure. J Adhes Sci Technol 2012;26(4-5):447–61.
[2] Cucchiella F, Dadamo I. Estimation of the energetic and environmental impacts of a roof-mounted building-integrated photovoltaic systems. Renew Sust Energ Rev 2012;16(7):5245–59.
[3] Levin T, Thomas VM, Lee AJ. State-scale evaluation of renewable electricity policy: The role of renewable electricity credits and carbon taxes. Energy Policy 2010;39(2):950–60.
[4] Liu W, Lund H, Mathiesen BV, Zhang X. Potential of renewable energy systems in China. Appl Energy 2011;88(2):518–25.
[5] Hofman K, Li X. Canada's energy perspective and policies for sustainable development. Appl Energy 2009;86(4):407–15.
[6] US Energy Information Administration. International Energy Outlook. 2010. Washington, DC: U.S. Department of Energy.
[7] Lloyd B, Forest AS. The transition to renewables: Can PV provide an answer to the peak oil and climate change challenges? Energy Policy 2010;38(11):7378–94.
[8] Apergis N, Payne JE. A global perspective on the renewable energy consumption-growth nexus. Energy Source Part B 2012;7(3):314–22.
[9] Kaygusuz K. Energy for sustainable development: Key issues and challenges. Energy Source Part B 2007;2(1):73–83.
[10] United Nations Development Program. World Energy Assessment: Energy and the challenge of sustainability. United Nations. 2000; Goldemberg, J. ed: New York.
[11] Dalili N, Edrisy A, Carriveau R. A review of surface engineering issues critical to wind turbine performance. Renew Sust Energy Rev 2009;13(2):428–38.
[12] Makkonen L, Laakso T, Marjaniemi M, Finstad KJ. Modeling and prevention of ice accretion on wind turbines. Wind Eng 2001;25(1):3–21.
[13] Botta G, Cavaliere M, Viani S, Pospíšil S. Effects of hostile terrains on wind turbine performance and loads: the AcquaSpruzzaexperience. J Wind Eng Ind Aerod 1998;74-76:419–31.
[14] Menini R, Farzaneh M. Elaboration of Al_2O_3/PTFE icephobic coatings for protecting aluminum surfaces. Surf Coat Tech 2009;203(14):1941–6.
[15] Kulinich SA, Farzaneh M. Ice adhesion on super-hydrophobic surfaces. Appl Surf Sci 2009;255(18):8153–7.
[16] Varanasi KK, Deng T, Smith JD, Hsu M, Bhate N. Frost formation and ice adhesion on superhydrophobic surfaces. Appl Phys Lett 2010;97:23.
[17] Nakajima A. Design of a transparent hydrophobic coating. J Ceram Soc Jpn 2004;112(1310):533–40.
[18] Extrand CW. Model for contact angles and hysteresis on rough and ultraphobic surfaces. Langmuir 2002;18(21):7991–9.
[19] Nosonovsky M, Bhushan B. Hierarchical roughness optimization for biomimetic superhydrophobic surfaces. Ultramicroscopy 2007;107(10-11):969–79.
[20] Barthlott W, Neinhuis C. Purity of the sacred lotus, or escape from contamination in biological surfaces. Planta 1997;202(1):1–8.
[21] Neinhuis C, Barthlott W. Characterization and distribution of water-repellent, self-cleaning plant surfaces. Ann Botany 1997;79(6):667–77.
[22] Yan YY, Gao N, Barthlott W. Mimicking natural superhydrophobic surfaces and grasping the wetting process: A review on recent progress in preparing superhydrophobic surfaces. Adv Colloid Interfac 2011;169(2):80–105.
[23] Law M, Greene LE, Johnson JC, Saykally R, Yang P. Nanowire dye-sensitized solar cells. Nature Mater 2005;4(6):455–9.
[24] Xu F, Dai M, Lu Y, Sun L. Hierarchical ZnO nanowire-nanosheet architectures for high power conversion efficiency in dye-sensitized solar cells. J Phys Chem C 2010;114(6):2776–82.
[25] Geim AK, Dubonos SV, Grigorieva IV, Novoselov KS, Zhukov AA, Shapoval SY. Microfabricated adhesive mimicking gecko foot-hair. Nature Mater 2003;2(7):461–3.
[26] Lee H, Lee BP, Messersmith PB. A reversible wet/dry adhesive inspired by mussels and geckos. Nature 2007;448(7151):338–41.
[27] Liu SY, Zhang P, Lü H, Zhang CW, Xia Q. Fabrication of high aspect ratio microfiber arrays that mimic gecko foot hairs. Chin Sci Bull 2012;57(4):404–8.
[28] Spolenak R, Gorb S, Arzt E. Adhesion design maps for bio-inspired attachment systems. Acta Biomater 2005;1(1):5–13.
[29] Dalsin JL, Hu B, Lee BP, Messersmith PB. Mussel adhesive protein mimetic polymers for the preparation of nonfouling surfaces. J Am Chem Soc 2003;125(14):4253–8.
[30] Potyrailo RA, Ghiradella H, Vertiatchikh A, Dovidenko K, Cournover JR, Olson E. Morpho butterfly wing scales demonstrate highly selective vapor response. Nature Photon 2007;1(2):123–8.
[31] Huang J, Wang X, Wang ZL. Controlled replication of butterfly wings for achieving tunable photonic properties. Nano Lett 2006;6(10):2325–31.
[32] Parker AR, Townley HE. Biomimetics of photonic nanostructures. Nat Nanotechnol 2007;2(6):347–53.
[33] Srinivasarao M. Nano-optics in the biological world: Beetles, butterflies, birds, and moths. Chem Rev 1999;99(7):1935–61.
[34] Vukusic P, Sambles JR. Photonic structures in biology. Nature 2003;424(6950):852–5.
[35] Min W, Jiang B, Jiang P. Bioinspired self-cleaning antireflection coatings. Adv Mater 2008;20(20):3914–8.
[36] Wu D, Chen Q, Xia H, Jiao J, Xu B, Lin X, et al. A facile approach for artificial biomimetic surfaces with both superhydrophobicity and iridescence. Soft Matter 2010;6(2):263–7.
[37] Li Y, Zhang J, Zhu S, Dong. H, Jia F, Wang Z, et al. Biomimetic surfaces for high-performance optics. Adv Mater 2009;21(46):4731–4.
[38] Hou W, Wang Q. Stable polytetrafluoroethylenesuperhydyrophobic surface with lotus-leaf structure. J Colloid Interfac 2009;333(1):400–3.
[39] Bhushan B, Koch K, Jung YC. Biomimetic hierarchical structure for self-cleaning. App Phys Lett 2008;93:9.
[40] Koch K, Barthlott W. Superhydrophobic and superhydrophilic plant surfaces: An inspiration for biomimetic materials. Phil Trans R Soc A 2009;367(1893):1487–509.
[41] Sun T, Feng L, Gao X, Jiang L. Bioinspired surfaces with special wettability. Acc Chem Res 2005;38(8):644–52.
[42] Gao X, Jiang L. Water-repellent legs of water striders. Nature 2004;432(7013):36.
[43] Lee W, Jin M, Yoo W, Lee J. Nanostructuring of a polymeric substrate with well-defined nanometer-scale topography and tailored surface wettability. Langmuir 2004;20(18):7665–9.
[44] Guo Z, Liu W, Su B. Superhydrophobic surfaces: From natural to biomimetic to functional. J Colloid Interfac 2011;353(2):335–55.
[45] Feng L, Li S, Li Y, Li H, Zhang L, Zhai J, et al. Super-hydrophobic surfaces: From natural to artificial. Adv Mater 2002;14(24):1857–60.
[46] Gao J, Liu Y, Xu H, Wang Z, Zhang X. Mimicking biological structured surfaces by phase-separation micromolding. Langmuir 2009;25(8):4365–9.
[47] Gao J, Liu Y, Xu H, Wang Z, Zhang X. Biostructure-like surfaces with thermally responsive wettability prepared by temperature-induced phase separation micromolding. Langmuir 2010;26(12):9673–6.
[48] Lin J, Cai Y, Wang X, Ding B, Yu J, Wang M. Fabrication of biomimetic superhydrophobic surfaces inspired by lotus leave and silver ragwort leaf. Nanoscale 2011;3(3):1258–62.
[49] Solga A, Cerman Z, Striffler BF, Spaeth M, Barthlott W. The dream of staying clean: Lotus and biomimetic surfaces. Bioinspir Biomim 2007;2(4):S126–34.
[50] Young T. An essay on the cohesion of fluids. Phil Trans R Soc London 1805;95:65–87.
[51] Wenzel RN. Resistance of solid surfaces to wetting by water. Ind Eng Chem Res 1936;28(8):988–94.
[52] Wenzel RN. Surface roughness and contact angle. J Phys Colloid Chem 1949;53(9):1466–7.
[53] Cassie ABD, Baxter S. Wettability of porous surfaces. Trans Farad Soc 1944;40:546–51.
[54] Cassie ABD. Contact angles. Discuss Farad Soc 1948;3:11–6.
[55] Krasowska M, Zawala J, Malysa K. Air at hydrophobic surfaces and kinetics of three phase contact formation. Adv Colloid Interfac 2009;147-148(C):155–69.

[56] Kavale MS, Mahadik DB, Parale VG, Wagh PB, Gupta SC, Rao AV, et al. Optically transparent, superhydrophobicmethyltrimethoxysilane based silica coatings without silylating reagent. Appl Surf Sci 2011;258(1):158–62.
[57] Hare EF, Shafrin EG, Zisman WA. Properties of films of adsorbed fluorinated acids. J Phys Chem 1954;58(3):236–9.
[58] Nishino T, Meguro M, Nakamae K, Matsushita M, Ueda Y. The lowest surface free energy based on –CF3 alignment. Langmuir 1999;15(13):4321–3.
[59] Dodiuk H, Rios PF, Dotan A, Kenig S. Hydrophobic and self-cleaning coatings. Polymer Adv Tech 2007;18(9):746–50.
[60] Gao N, Yan YY, Chen XY, Mee DJ. Superhydrophobic surfaces with hierarchical structure. Mater Lett 2011;65(19-20):2902–5.
[61] Nosonovsky M. Multiscale roughness and stability of superhydrophobic biomimetic interfaces. Langmuir 2007;23(6):3157–61.
[62] Zhao N, Xu J, Xie Q, Weng L, Guo X, Zhang X, et al. Fabrication of biomimetic superhydrophobic coating with a micro-nano-binary structure. Macrocol Rapid Commun 2005;26(13):1075–80.
[63] Bhushan B, Jung YC, Koch K. Micro-, nano-, and hierarchical structures for superhydrophobicity, self-cleaning and low adhesion. Phil Trans R Soc A 2009;367(1894):1631–72.
[64] Rios PF, Dodiuk H, Kenig S, McCarthy S, Dotan A. The effects of nanostructure and composition on the hydrophobic properties of solid surface. J Adhes Sci Technol 2006;20(6):563–87.
[65] Rios PF, Dodiuk H, Kenig S, McCarthy S, Dotan A. Transparent ultrahydrophobic surfaces. J Adhes Sci Technol 2007;21(5-6):399–408.
[66] Wu Y, Inoue Y, Sugimura H, Takai O, Kato H, Murai S, et al. Characteristics of ultra water-repellent thin films prepared by combined process of microwave plasma-enhanced CVD and oxygen-plasma treatment. Thin Solid Films 2002;407(1-2):45–9.
[67] Miyahara Y, Mitamura K, Saito N, Takai O. Fabrication of microtemplates for the control of bacterial immobilization. J Vac Sci Technol A. 2009;27(5):1183–7.
[68] Intravuovo F, Sardella E, Rossini P, D'Agostino R, Favia P. PECVD of fluorocarbon coatings from hexafluoropropylene oxide: Glow vs. afterglow. Chem Vap Deposition 2009;15(4-6):95–100.
[69] Milella A, Di Mundo R, Palumbo F, Favia P, Fracassi F, D'Agostino R. Plasma nanostructuring of polymers: Different routes to superhydrophobicity. Plasma Processes Polym 2009;6(6-7):460–6.
[70] Sarkar DK, Farzaneh M. Superhydrophobic coatings with reduced ice adhesion. J Adhes Sci Tech 2009;23(9):1215–37.
[71] Fang X, Yu Z, Sun X, Liu X, Qin F. Formation of supherhydrophobicboehmite film on glass substrate by sol-gel method. Front Chem Eng Chin 2009;3(1 SPEC.ISS):97–101.
[72] Mahadik SA, Kavale MS, Mukherjee SK, Rao AV. Transparent superhydrophobic silica coatings on glass by sol-gel method. Appl Surf Sci 2010;257(2):333–9.
[73] Latthe SS, Imai H, Ganesan V, Rao AV. Porous superhydrophobic silica films by sol-gel process. MicroporousMesoporous Mater 2010;130(1-3):115–21.
[74] Latthe SS, Imai H, Ganesan V, Rao AV. Superhydrophobic silica films by sol-gel co-precursor method. Appl Surf Sci 2009;256(1):217–22.
[75] Ganbavle VV, Bangi UKH, Latthe SS, Mahadik SA, Rao AV. Self-cleaning silica coatings on glass by single step sol-gel route. Surf Coat Technol 2011;205(23-24):5338–44.
[76] Manca M, Cannavale A, De Marco L, Aricò AS, Cingolani R, Gigli G. Durable superhydrophobic and antireflective surfaces by trimethylsilanizedsilicanano particles-based sol-gel processing. Langmuir 2009;25(11):6357–62.
[77] Shang HM, Wang Y, Limmer SJ, Chou TP, Takahashi K, Cao GZ. Optically transparent superhydrophobicsilica-based films. Thin Solid Films 2005;472(1-2):37–43.
[78] Lim H, Jung D, Noh J, Choi G, Kim W. Simple nanofabrication of asuperhydrophobic and transparent biomimetic surface. Chin Sci Bull 2009;54(19):3613–6.
[79] Choi C, Ulmanella U, Kim J, Ho C, Kim C. Effective slip and friction reduction in nanogratedsuperhydrophobicmicrochannels. Phys Fluids 2006;18:8.
[80] Kwon Y, Patankar N, Choi J, Lee J. Design of surface hierarchy for extremehydrophobicity. Langmuir 2009;25(11):6129–36.
[81] Song W, Veiga DD, Custódio CA, Mano JF. Bioinspireddegradablesubstrateswithextremewettabilityproperties. Adv Mater 2009;21(18):1830–4.
[82] Lee Y, Ju K, Lee J. Stable biomimeticsuperhydrophobic surfaces fabricated by polymerreplicationmethodfromhierarchicallystructured surfaces of al templates. Langmuir 2010;26(17):14103–10.
[83] Yuan Z, Chen H, Tang J, Gong H, Liu Y, Wang Z, et al. A novelpreparation of polystyrene film withasuperhydrophobic surface using a templatemethod. J Phys D: Appl Phys 2007;40(11):3485–9.
[84] Hwang HS, Kim NH, Lee SG, Lee DY, Cho K, Park I. Facile fabrication of transparent superhydrophobic surfaces by spray deposition. ACS Appl Mater Interfaces 2011;3(7):2179–83.
[85] Tarwal NL, Patil PS. Superhydrophobic and transparent ZnO thin films synthesized by spray pyrolysis technique. Appl Surf Sci 2010;256(24):7451–6.
[86] Patil PS. Versatility of chemical spray pyrolysis technique. Mater Chem Phys 1999;59(3):185–98.
[87] Li X, Du X, He J. Self-cleaning antireflective coatings assembled from peculiar mesoporous silica nanoparticles. Langmuir 2010;26(16):13528–34.
[88] Liao K, Wan A, Batteas JD, Bergbreiter DE. Superhydrophobic surfaces formed using layer-by-layer self-assembly with aminated multiwall carbon nanotubes. Langmuir 2008;24(8):4245–53.
[89] Li Y, Liu F, Sun J. A facile layer-by-layer deposition process for the fabrication of highly transparent superhydrophobic coatings. Chem Commun 2009;19:2730–2.
[90] Kim T, Baek CH, Suh KY, Seo S, Lee HH. Optical lithography with printed metal mask and a simple superhydrophobic surface. Small 2008;4(2):182–5.
[91] He B, Lee J, Patankar NA. Contact angle hysteresis on rough hydrophobic surfaces. Colloids Surf. A 2004;248(1-3):101–4.
[92] Wang JZ, Zheng ZH, Li HW, Huck WTS, Sirringhaus H. Dewetting of conducting polymer inkjet droplets on patterned surfaces. Nat Mater 2004;3(3):171–6.
[93] Fürstner R, Barthlott W, Neinhuis C, Walzel P. Wetting and self-cleaning properties of artificial superhydrophobic surfaces. Langmuir 2005;21(3):956–61.
[94] Fletcher. NH. The Chemical Physics of Ice. Cambridge, Great Britain: Cambridge University Press; 1970.
[95] Wilson PW, Heneghan AF, Haymet ADJ. Ice nucleation in nature: Supercooling point (SCP) measurements and the role of hetergeneous nucleation. Cryobiology 2003;46(1):88–9.
[96] Makkonen L. Models for the growth of rime, glaze, icicles and wet snow on structures. Phil Trans R Soc A 2000;358(1776):2913–39.
[97] Petrie EM. Strategies for combating ice adhesion. Evaluating application-specific methods that help ensure smooth function of the world's infrastructure. Met Finish 2009;107(2):56–9.
[98] Huang Y, Hu M, Yi S, Liu X, Li H, Huang C, et al. Preparation and characterization of silica/fluorinated acrylate copolymers hybrid films and the investigation of their icephobicity. Thin Solid Films. 2012;520(17):5644–51.
[99] Alizadeh A, Yamada M, Li R, Shang W, Otta S, Zhong S, et al. Dynamics of ice nucleation on water repellent surfaces. Langmuir 2012;28(6):3180–6.
[100] Tourkine P, Merrer ML, Quéré D. Delayedfreezing on water repellentmaterials. Langmuir 2009;25(13):7214–6.
[101] Sarshar MA, Swarctz C, Hunter S, Simpson J, Choi CH. Effects of contact angle hysteresis on iceadhesion and growth on superhydrophobic surfaces underdynamic flow conditions. Colloid Polym Sci 2013;291:427–35.
[102] Antonini C, Innocenti M, Horn T, Marengo M, Amirfazli A. Understanding the effects of superhydrophobiccoatings on energyreduction in anti-icingsystems. Cold Reg Sci Technol 2011;67(1-2):58–67.
[103] Wang H, He G, Tian Q. Effects of nano-fluorocarboncoatings on icing. Appl Surf Sci 2012;258(18):7219–24.
[104] Meuler AJ, Smith JD, Varanasi KK, Mabry JM, McKinley GH, Cohen RE. Relationship between water wettability and ice adhesion. ACS Appl Mater Interfaces 2010;2(11):3100–10.
[105] Kulinich SA, Farzaneh M. How wetting hysteresis influences ice adhesion strength on superhydrophobic surfaces. Langmuir 2009;25(16):8854–6.
[106] Kulinich SA, Farzaneh M. On ice-releasing properties of rough hydrophobic coatings. Cold Reg Sci Technol 2011;65(1):60–4.
[107] Nosonovsky M, Hejazi V. Why superhydrophobic surfaces are not alwaysicephobic. ACS Nano 2012;6(10):8488–91.
[108] Kulinich SA, Farhadi S, Nose K, Du XW. Superhydrophobic surfaces: Are they really ice-repellent? Langmuir 2011;27(1):25–9.
[109] Ryzhkin IA, Petrenko VF. Physical mechanisms responsible for ice ahesion. J Phys Chem B 1997;101(32):6267–70.
[110] Saleema N, Farzaneh M, Paynter RW, Sarkar DK. Prevention of ice accretion on aluminum surfaces by enhancing their hydrophobic properties. J Adhes Sci Technol 2011;25(1-3):27–40.
[111] Cao L, Jones AK, Sikka VK, Wu J, Gao D. Anti-icing superhydrophobic coatings. Langmuir 2009;25(21):12444–48.
[112] Furuta T, Sakai M, Isobe T, Nakajima A. Effect of dew condesation on the wettability of rough hydrophobic surfaces coated with two different silanes. Langmuir 2010;26(16):13305–9.
[113] Karmouch R, Ross GG. Experimental study on the evolution of contact angles with temperature near the freezing point. J Phys Chem C 2010;114(9):4063–6.
[114] Meuler AJ, McKinley GH, Cohen RE. Exploiting topographical texture to impart icephobicity. ACS Nano 2010;4(12):7048–52.
[115] Wang F, Li C, Lv Y, Lv F, Du Y. Ice accretion on superhydrophobic aluminum surfaces under low-temperature conditions. Cold Reg Sci Technol 2010;62(1):29–33.
[116] Liu Z, Gou Y, Wang J, Cheng S. Frost formation on a superhydrophobic surface under natural convection conditions. Int J Heat Mass Transfer 2008;51(25-26):5975–82.
[117] Cai L, Wang R, Hou P, Zhang X. Study on restraining frost growth at initial stage by hydrophobic coating and hygroscopic coating. Energy Build 2011;43(5):1159–63.
[118] Kako T, Nakajima A, Kato Z, Uematsu K, Watanabe T, Hashimoto K. Adhesion and sliding of snow on hydrophobic solid surface. J Ceram Soc Jpn 2002;110(1279):186–92.
[119] Chen J, Liu J, He M, Li K, Cui D, Zhang Q, et al. Superhydrophobic surfaces cannot reduce ice adhesion. Appl Phys Lett 2012;101:11.
[120] Jafari R, Menini R, Farzaneh M. Superhydrophobic and icephobic surfaces prepared by RF-sputtered polytetrafluoroethylene coatings. Appl Surf Sci 2010;257(5):1540–3.
[121] Menini R, Ghalmi Z, Farzaneh M. Highly resistant icephobic coatings on aluminum alloys. Cold Reg Sci Technol 2010;65(1):65–9.
[122] Farhadi S, Farzaneh M, Kulinich SA. Anti-icing performance of superhydrophobic surfaces. Appl Surf Sci 2011;257(14):6264–9.

[123] Wang Y, Xue J, Wang Q, Chen Q, Ding J. Verification of icephobic/anti-icing properties of a superhydrophobic surface. ACS Appl Mater Interface 2013;5:3370–81.
[124] Dodiuk H, Kenig S, Dotan A. Do self-cleaning surfaces repel ice? J Adhes Sci Technol 2012;26(4-5):701–14.
[125] Cho KL, Liaw II, Wu AH, Lamb RN. Influence of roughness on a transparent superhydrophobic coating. J Phys Chem C 2010;114(25):11228–33.
[126] Xu L, Karunakaran RG, Guo J, Yang S. Transparent, superhydrophobic surfaces from one-step spin coating of hydrophobic nanoparticles. ACS Appl Mater Interfaces 2012;4(2):1118–25.
[127] Deng X, Mammen L, Zhao Y, Lellig P, Müllen K, Li C, et al. Transparent, thermally stable and mechanically robust superhydrophobic surfaces made from porous silica capsules. Adv Mater 2011;23(26):2962–5.
[128] Bravo J, Zhai L, Wu Z, Cohen RE, Rubner MF. Transparent superhydrophobic films based on silica nanoparticles. Langmuir 2007;23(13):7293–8.
[129] Verma LK, Sakhuja M, Son J, Danner AJ, Yang H, Zeng HC, et al. Self-cleainging and anitreflective packaging glass for solar modules. Renewable Energy 2011;36(9):2489–93.
[130] Wang J, Wang L, Feng L. One-step fabrication of fluoropolymer transparent films with superhydrophobicity by dry method. J Appl Polym Sci 2011;120 (1):524–9.
[131] Yabu H, Shimomura M. Single-step fabrication of transparent superhydrophobic porous polymer films. Chem Mater 2005;17(21):5231–4.
[132] Takeda K, Sasaki M, Kieda N, Katayama K, Kako T, Hashimoto K, et al. Preparation of transparent super-hydrophobic polymer film with brightness enhancement property. J Mater Sci Lett 2001;20(23):2131–3.
[133] Gao L, He J. A facile dip-coating approach based on three silica sols to fabrication of broadband antireflective superhydrophobic coatings. J Colloid Interfac Sci 2013;400:24–30.
[134] Li X, He J, Liu W. Broadband anti-reflective and water-repellent coatings on glass substrates for self-cleaning photovoltaic cells. Mater Res Bull 2013;48:2522–8.
[135] Gao L, He J. Surface hydrophobic co-modification of hollow silica nanoparticles toward large-area transparent superhydrophobic coatings. J Colloid Interface Sci 2013;396:152–9.
[136] Zhu J, Hsu C, Yu Z, Fan S, Cui Y. Nanodome solar cells with efficient light management and self-cleaning. Nano Lett 2010;10(6):1979–84.
[137] Choi S, Huh S. Direct structuring of a biomimetic anitreflective, self-cleaning surface for light harvesting in organic solar cells. Macromol Rapid Commun 2010;31(6):539–44.
[138] Blossey R. Self-cleaning surfaces – virtual realities. Nat Mater 2003;2 (5):301–6.
[139] Xiu Y, Zhang S, Yelundur V, Rohathi A, Hess DW, Wong CP. Superhydrophobic and low light reflectivity silicon surfaces fabricated by hierarchical etching. Langmuir 2008;24(18):10421–6.
[140] Lee D, Rubner MF, Cohen RE. All-nanoparticle thin-film coatings. Nano Lett 2006;6(10):2305–12.
[141] Ling XY, Phang IY, Vansco GJ, Huskens J, Reinhoudt DN. Stable and transparent superhydrophobic nanoparticle films. Langmuir 2009;25 (5):3260–3.
[142] Prado R, Beobide G, Marcaide A, Goikoetxea J, Aranzabe A. Development of multifunctional sol-gel coatings: Anti-reflection coatings with enhanced self-cleaning capacity. Sol Energy Mater Sol Cells 2010;94(6):1081–8.
[143] Son J, Kundu S, Verma LK, Sakhuja M, Danner AJ, Bhatia CS, et al. A practical superhydrophilic self cleaning and antireflective surface for outdoor photovoltaic applications. Sol Energy Mater Sol Cells 2012;98:46–51.
[144] Cao M, Song X, Zhai J, Wang J, Wang Y. Fabrication of highly anitreflective silicon surfaces with superhydrophobicity. J Phys Chem B 2006;110 (26):13072–5.
[145] Zhang X, Fujishima A, Jin M, Emeline AV, Murakami T. Double-layered TiO_2-SiO_2 nanostructured films with self-cleaning and antireflective properties. J Phys Chem B 2006;110(50):25142–8.
[146] Zhang X, Sato O, Taguchi M, Einaga Y, Murakami T, Fujishima A. Self-cleaning particle coating with antireflection properties. Chem Mater 2005;17 (3):696–700.
[147] Suresh Kumar P, Sundaramurthy J, Mangalaraj D, Nataraj D, Rajarathnam D, Srinivasan MP. Enhanced super-hydrophobic and switching behavior of ZnO nanostructured surfaces prepared by simple solution – immersion successive ionic layer adsoroption and reaction process. J Colloid Interface Sci 2011;363 (1):51–8.
[148] Park MS, Lee Y, Kim JK. One-step preparation of antireflection film by spin-coating of polymer/solvent/nonsolvent ternary system. Chem Mater 2005;17 (15):3944–50.
[149] Minemoto T, Mizuta T, Takakura H, Hamakawa Y. Antireflective coating fabricated by chemical deposition of ZnO for spherical Si solar cells. Sol Energy Mater Sol Cells 2007;91(2-3):191–4.
[150] Schirone L, Sotgui G, Califano FP. Chemically etched porous silicon as an anit-reflection coating for high efficiency solar cells. Thin Solid Films 1997;297(1-2):296–8.
[151] Xiong J, Das SN, Shin B, Kar JP, Choi JH, Myoung J. Biomimetic hierarchical ZnO structure with superhydrophobic and antireflective properties. J Colloid Interface Sci 2010;350(1):344–7.
[152] Swatowska B, Stapinski T, Drabczyk K, Panek P. The role of antireflective coatings in silicon solar cells – the influence on their electrical parameters. Optica Applicata 2011;41(2):487–92.
[153] Lin GJ, Lai KY, Lin CA, Lai Y, He JH. Efficiency enhancement of InGaN-based multiple quantum well solar cells employing antireflective ZnOnanorod arrays. IEEE Electron Device Lett 2011;32(8):1104–6.
[154] Prevo BG, Hon EW, Velev OD. Assembly and characterization of colloid-based antireflective coatings on multicrystalline silicon solar cells. J Mater Chem 2007;17(8):791–9.
[155] Verho T, Bower C, Andrew P, Franssila S, Ikkala O, Ras RHA. Mechanically durable superhydrophobic surfaces. Adv Mater 2011;23(5):673–8.
[156] Marquez-Velasco J, Vlachopoulou M, Tserepi A, Gogolides E. Stable superhydrophobic surfaces induced by dual-scale topography on SU-8. Microelectron Eng 2010;87(5-8):782–5.
[157] Guo L, Yuan W, Li J, Zhang Z, Xie Z. Stable superhydrophobic surfaces over a wide pH range. Appl Surf Sci 2008;254(7):2158–61.
[158] Rao AV, Latthe SS, Mahadik SA, Kappenstein C. Mechanically stable and corrosion resistant superhydrophobic sol-gel coatings on copper substrate. Appl Surf Sci 2011;257(13):5772–6.
[159] Xue CH, Ma JZ. Long-lived superhydrophobic surfaces. J Mater Chem A 2013;1:4146–61.
[160] Sasaki M, Kieda N, Katayama K, Takeda K, Nakajima A. Processing and properties of transparent super-hydrophobic polymer film with low surface electric resistance. J Mater Sci 2004;39(11):3717–22.
[161] Nakajima A, Hashimoto K, Watanabe T, Takai K, Yamauchi G, Fujishima A. Transparent superhydrophobic thin films with self-cleaning properties. Langmuir 2000;16(17):7044–7.
[162] Boinovich LB, Emelyanenko AM, Ivanov VK, Pashinin AS. Durable icephobic coating for stainless steel. ACS Appl Mater Interfaces 2013;5:2549–54.
[163] Wang T, Isimjan TT, Chen J, Rohani S. Transparent nanostructured coatings with UV-shielding and superhydrophobicity properties. Nanotechnology 2011;22:26.